PLANT SCIENCE TODAY
Vol x(x): xx–xx
https://doi.org/10.14719/pst.9444

eISSN 2348-1900

RESEARCH ARTICLE

Spatial rice yield estimation using semi-physical and crop simulation models: A comparative approach

S Satheesh[1], Sellaperumal Pazhanivelan[2*], D Suresh Kumar[3], KP Ragunath[2], R Kumaraperumal[1], AP Sivamurugan[4], D Muthumanickam[1], NS Sudarmanian[2] & S Sakthivel[4]

[1]Department of Remote Sensing and GIS, Tamil Nadu Agricultural University, Coimbatore 641 003, Tamil Nadu, India
[2]Centre for Water and Geospatial Studies, Tamil Nadu Agricultural University, Coimbatore 641 003, Tamil Nadu, India
[3]Centre for Agricultural and Rural Development Studies, Tamil Nadu Agricultural University, Coimbatore 641 003, Tamil Nadu, India
[4]Department of Agronomy, Tamil Nadu Agricultural University, Coimbatore 641 003, Tamil Nadu, India

*Correspondence email - pazhanivelans@gmail.com

Received: 15 May 2025; Accepted: 14 June 2025; Available online: Version 1.0: 13 July 2025

Cite this article: Satheesh S, Sellaperumal P, Suresh DK, Ragunath KP, Kumaraperumal R, Sivamurugan AP, Muthumanickam D, Sudarmanian NS, Sakthivel S. Spatial rice yield estimation using semi-physical and crop simulation models: A comparative approach. Plant Science Today (Early Access). https://doi.org/10.14719/pst.9444

Abstract

This study presents a comparative assessment of two modelling approaches for estimating spatial rice yields across the Cauvery delta zone (CDZ) in Tamil Nadu, viz., (a) a process-based crop simulation model (DSSAT-CERES Rice) and (b) a semi-physical model (SPM). The DSSAT model was calibrated using field data, cultivar-specific genetic coefficients and further refined through the integration of leaf area index (LAI) derived from Sentinel-1 synthetic aperture radar (SAR) imagery. In contrast, the SPM utilized remote sensing-derived inputs such as photosynthetically active radiation (PAR), fraction of absorbed PAR (FPAR), temperature and water stress indices and radiation use efficiency (RUE) to compute yield via net primary productivity (NPP). Results revealed that DSSAT achieved higher alignment with crop cutting experiment (CCE) data (88.6 %) than SPM (83.3 %), attributed to its capability to simulate complex crop-soil-climate interactions. However, the SPM demonstrated greater scalability and ease of implementation, particularly in regions with limited field data. The study highlights the strengths and limitations of each approach, offering insights into model selection based on accuracy, data availability and operational feasibility. These findings suggest that integration of remote sensing and crop modelling could serve as a valuable strategy for improving regional yield forecasting and enhancing agricultural decision-making.

Keywords: DSSAT; FPAR; rice area; SAR; semi-physical model; spatial yield

Introduction

Timely and accurate crop yield estimation is essential for ensuring food security, resource optimization and effective policy making (1). Rice (*Oryza sativa* L.), the staple food for over half the global population, holds significant socioeconomic importance, especially across Asia (2). The demand for scalable, data-driven yield estimation techniques has grown significantly in response to the challenges posed by climate change, scarce resources and changing land use (3).

Traditional forecasting methods, largely based on field surveys and expert judgment, are often time-consuming, labour-intensive and expensive. To address these limitations, the integration of remote sensing and crop modelling has emerged as a powerful alternative, enabling large-scale, cost-effective and timely yield assessments (4).

Among various remote sensing (RS) based yield forecasting models, two prominent modelling approaches are semi-physical models and process-based crop simulation models. Semi-physical models use remote sensing-derived inputs such as photosynthetically active radiation (PAR), fraction of absorbed photosynthetically active aadiation (FPAR), temperature and water stress to estimate yield based on biophysical relationships. They are easier to implement, computationally efficient and useful in data-scarce regions. Synthetic aperture radar (SAR)-derived metrics in a semi-physical framework to estimate rice yields over large areas (5). Process-based crop models like DSSAT simulate physiological crop processes by integrating genotype, environment and management (G × E × M) interactions. Although more accurate and adaptable to diverse agro-climatic conditions, these models require extensive input data and calibration (6). Remote sensing, particularly SAR (Sentinel-1), provides consistent, cloud-penetrating observations that complement both modelling approaches. SAR backscatter data are sensitive to crop structure and moisture, offering robust indicators of crop growth (7).

The present study provides a thorough comparative evaluation of the semi-physical model alongside the DSSAT crop simulation model for spatially estimating rice yield. The analysis utilizes remote sensing-derived biophysical indicators, ground truth data and environmental variables to assess each model's performance in terms of spatial accuracy, sensitivity and operational feasibility. By systematically contrasting these two modelling paradigms, this research contributes to the development of efficient, scalable and context-specific yield estimation frameworks, supporting advances in precision agriculture, climate-resilient farming, crop insurance companies and regional food security planning.

Materials and Methods

Study area

The Cauvery delta zone (CDZ), located in eastern Tamil Nadu, India, encompasses the districts of Thanjavur, Thiruvarur, Nagapattinam and Mayiladuthurai. Geographically, the region lies between 10°00′N and 11°15′N latitude and 78°45′E and 79° 55′E longitude, featuring flat terrain that gradually slopes toward the Bay of Bengal (Fig. 1). Agriculture in the CDZ is primarily supported by regulated irrigation from the Mettur Dam and seasonal rainfall, particularly from the northeast monsoon (October–December), which brings 900-1200 mm of annual precipitation. Rice is the dominant crop grown mainly during the *Kuruvai* (June-September), *Samba* (August-January) and *Thaladi* (October-February) seasons. Farming practices vary across districts, with Thanjavur and Thiruvarur possessing better irrigation infrastructure and mechanization, while Nagapattinam and Mayiladuthurai exhibit more traditional and diverse systems. The region's temperature ranges from 24 °C to 34 °C, which can accelerate crop development under heat stress. CDZ's agro-ecological diversity, variability in water availability and well-documented farming systems make it an ideal setting for comparative crop yield modelling. Its reliable remote sensing coverage and strong institutional support for ground-truth data further enhance its suitability for spatial analysis. The details of the satellite data used in this study are presented in Table 1.

Methodology for rice area estimation

The preprocessing of time-series Sentinel-1A SAR data, provided by ESA, was carried out using MAPscape-RICE-specialized software tailored by Sarmap, Switzerland. This customized tool incorporates a fully automated SAR processing workflow initially developed, specifically designed to convert multi-temporal Sentinel-1A IW-GRD SAR datasets into terrain-corrected σ° values (8) (Fig. 2). The processing steps were executed in the following sequence:

Strip mosaicking

SAR scenes from the same orbit and date were merged along the azimuth direction to create continuous image strips in slant range geometry, simplifying subsequent data processing.

Co-registration

All SAR images with consistent viewing geometry were co-registered to align pixels across acquisition dates, enabling effective multi-temporal analysis.

Time series speckle filtering

A temporal filter (equivalent number of looks) was applied to reduce speckle noise by assuming uniform surface reflectivity across time-series acquisitions.

Terrain geocoding, radiometric calibration and normalization

Using a DEM and a range-doppler approach, σ° backscatter was projected into SAR image space. Radiometric calibration accounted for antenna gain, scattering area and range spreading loss, while cosine-law correction normalized incidence angle variations.

ANLD filtering

An adaptive non-local means denoising filter enhanced spatial contrast by suppressing noise in homogeneous areas (9).

Atmospheric correction

An interpolation-based method corrected for atmospheric anomalies such as moisture-induced variations in the SAR signal (10).

Rice detection and classification

Post-processing, rice areas were identified using a rule-based classification in MAPscape-RIICE software. Temporal σ° backscatter profiles were analyzed based on local agronomic knowledge of rice phenology and cultivation practices. Although general detection rules were available, regional calibration was essential to adapt to local crop dynamics.

Methodology for spatial DSSAT yield estimation

The decision support system for agrotechnology transfer (DSSAT), developed through international cooperation under the IBSNAT initiative in the USA, was utilized in this study. Daily rice crop growth and development were modelled using CERES-Rice, a component of DSSAT version 4.7. The crop simulation model represents a simplified yet process-based framework to simulate crop growth and yield as influenced by interacting factors such as variety, soil properties, climatic conditions and management practices. In this study, the CERES-Rice model was successfully calibrated and validated to estimate rice yields across spatially heterogeneous environments within the CDZ.

Input requirements for the DSSAT model

Weather data

Weather data, including daily maximum and minimum temperatures (°C), solar radiation (MJ m^{-2}) and precipitation (mm), were formatted into DSSAT-compatible files using the built-in Weather Man utility for simulations with the CERES-Rice model.

Soil data

Soil profile information for Tamil Nadu was sourced from the Department of Remote Sensing and GIS, Tamil Nadu Agricultural University, at a 1:50,000 scale. This data was used to generate soil input files for DSSAT.

Table 1. Satellite data/products used in the study

S. No.	Satellite	Data/products	Resolution
1	INSAT 3DR	Daily insolation	1 km
2	MODIS	8 days composite FPAR	500 m
3	MODIS	8 days composite surface reflectance	500 m
4	Sentinel-1	Rice area mask	20 m
5	Gridded data	Daily minimum and maximum temperatures	5 km Grid

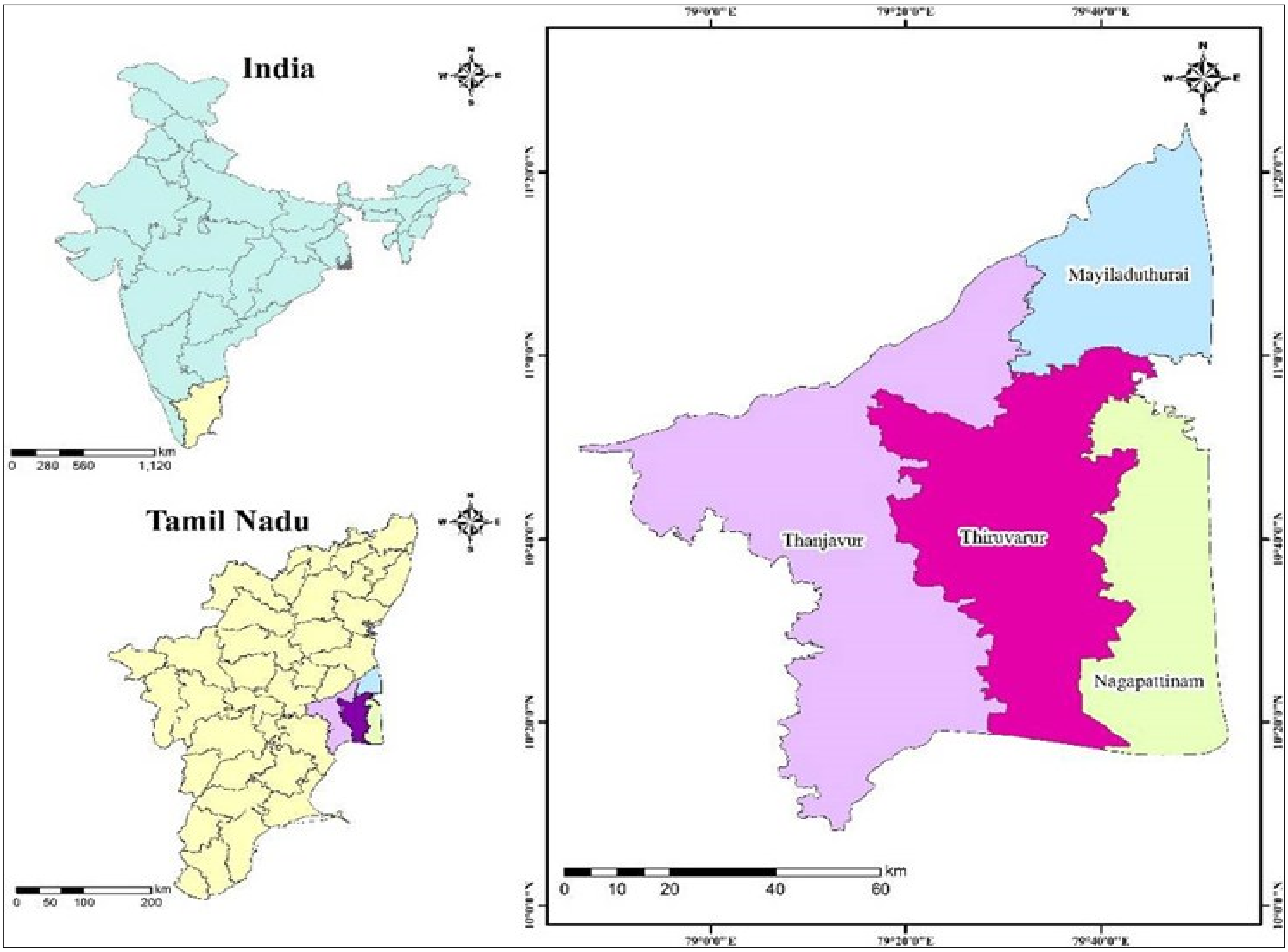

Fig. 1. Geographical location of the study area.

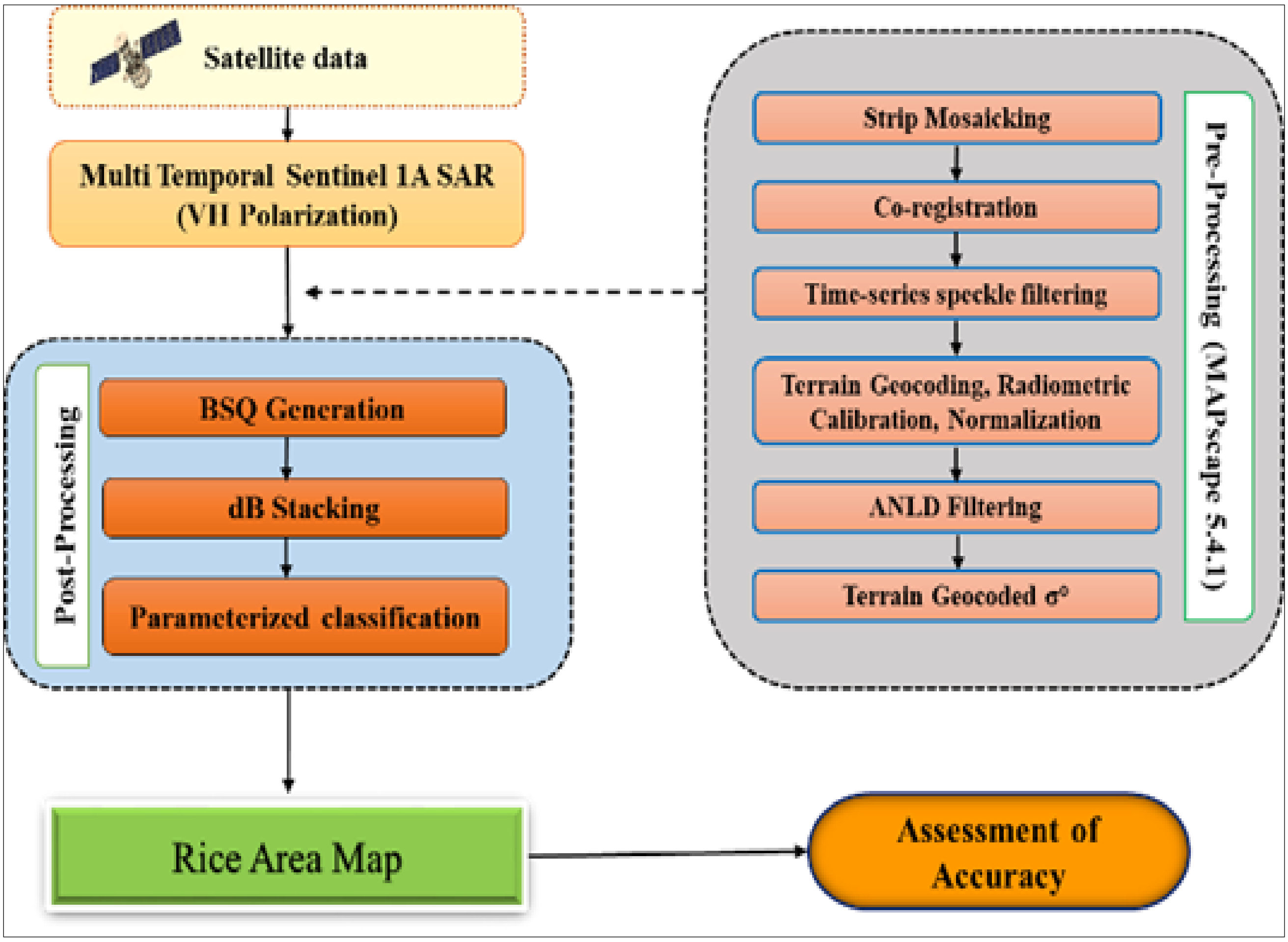

Fig. 2. Schematic representation of the processing of SAR data and rice area mapping.

Cultivar information

Genetic coefficient files for rice cultivars CR 1009, BPT 5204 and ADT 45 were prepared using field data

Crop management data

Using the 'X Build' tool in DSSAT, management files were created to capture detailed field conditions and experimental inputs. These included soil and field characteristics, planting configuration, irrigation and nutrient schedules, residue and chemical applications, tillage operations and simulation parameters.

Model calibration and validation

The model was calibrated with field data collected during the rice-growing season to estimate genetic coefficients for the three cultivars. Validation involved comparing simulated yields with actual yields recorded from farmers' fields in the study region. Model accuracy was evaluated using regression plots and correlation coefficients between observed and simulated outputs.

Derivation of leaf area index (LAI) from SAR backscatter data

Backscatter values in decibels (dB) were extracted from SAR images for selected monitoring fields using the QGIS point sampling tool. Simulated LAI values were paired with these dB values to establish a linear regression model. The QGIS raster calculator was then employed to generate spatial LAI maps by applying the regression equation to the dB images taken during the flowering stage of the rice crop.

Estimating rice yield through remote sensing

The final rice yield estimation combined DSSAT-simulated outputs with SAR-derived LAI data. A regression model was developed linking simulated yield and spatial LAI values derived from SAR imagery. This relationship was used to extrapolate rice yield across the broader study area (Fig. 3).

Methodology for semi physical approach yield estimation

Time series data downloaded from MOSDAC (INSAT 3DR) and MODIS satellite data from August 2024 to January 2025 were used for this analysis. The methodology for SPM is presented in Fig. 4.

Photosynthetically active radiation (PAR)

Insolation or incoming solar radiation, is the total amount of solar radiation received by an earth surface over a specific period. PAR is the portion of this solar radiation that falls within the 400-700 nm wavelength range, which is usable by plants for photosynthesis. PAR constitutes a fraction of the total insolation and is influenced by factors such as cloud cover, ozone levels and atmospheric conditions (11). Insolation data from the INSAT-3DR imager were downloaded for the study period. Daily insolation data was multiplied by 0.48 to generate daily PAR. Daily PAR is then composited into an 8-day composite raster with respect to the acquisition dates of the MODIS datasets. The datasets were resampled from 4000 m to 500 m.

Fraction of photosynthetically active radiation (FPAR)

FPAR quantifies the proportion of incoming PAR absorbed by the plant canopy, influenced by factors like canopy structure, leaf properties, atmospheric conditions and solar geometry. FPAR is linked to the plant's ability to synthesize carbohydrates and is crucial for estimating plant productivity (12). A well-growing crop with a dense canopy absorbs more PAR, resulting in higher FPAR values, while unhealthy vegetation reflects more PAR, leading to lower FPAR values. Higher FPAR generally leads to increased biomass and crop yield.

Computation of water stress

Water stress arises when a crop experiences insufficient water availability, negatively impacting its physiological functions. This water deficit occurs due to limited soil moisture, inadequate rainfall and excessive water loss through evapotranspiration. These processes are further influenced by atmospheric conditions, such as air saturation deficit (13). This imbalance affects physiological, morphological and biochemical processes, leading to reduced growth, yield and productivity. The SWIR (short wavelength infrared) band is sensitive to plant water content, making LSWI a valuable indicator of vegetation and soil moisture.

$$LSWI = \frac{NIR - SWIR}{NIR + SWIR} \qquad \text{(Eqn. 1)}$$

$$W_{stress} = \frac{1+LSWI}{1+LSWI_{max}} \qquad \text{(Eqn. 2)}$$

Where, W_{stress}= waer stress, LSWI = land surface water index, $LSWI_{max}$= maximum land surface water index of the area, NIR = near infrared and SWIR = short wavelength infrared.

Computation of temperature stress

Temperature data for the study area were retrieved in CSV format from the IMD data portal (14). The data were interpolated to generate a temperature raster. Temperature stress was generated using the equation:

$$T_{stress} = \frac{(T-T_{min})-(T-T_{max})}{(T-T_{min})(T-T_{max})(T-T_{0pt})2} \qquad \text{(Eqn. 3)}$$

Where, T_{stress} = temperature stress, T = daily mean temperature, T_{min} = minimum temperature for photosynthesis (°C), T_{max} = maximum temperature for photosynthesis (°C) and T_{opt} = optimum temperature for photosynthesis (°C).

Computation of net primary product (NPP)

NPP represents the rate at which an ecosystem accumulates biomass. Specifically, it is the difference between the amount of biomass crops produced through photosynthesis and the amount of energy (carbon dioxide) used for respiration (15).

RUE is the ratio of the biomass produced through photosynthesis to the amount of PAR intercepted by the plant (16). NPP for the period from sowing to harvest date has been computed at an interval of 8 days with a spatial resolution of 500 m using the periodical PAR, FPAR, W_{stress}, T_{stress} and maximum radiation use efficiency.

$$NPP = PAR \times FPAR \times RUE \times W_{stress} \times T_{stress} \qquad \text{(Eqn. 4)}$$

Total NPP has been computed for the whole rice growing season from 8-day composite datasets.

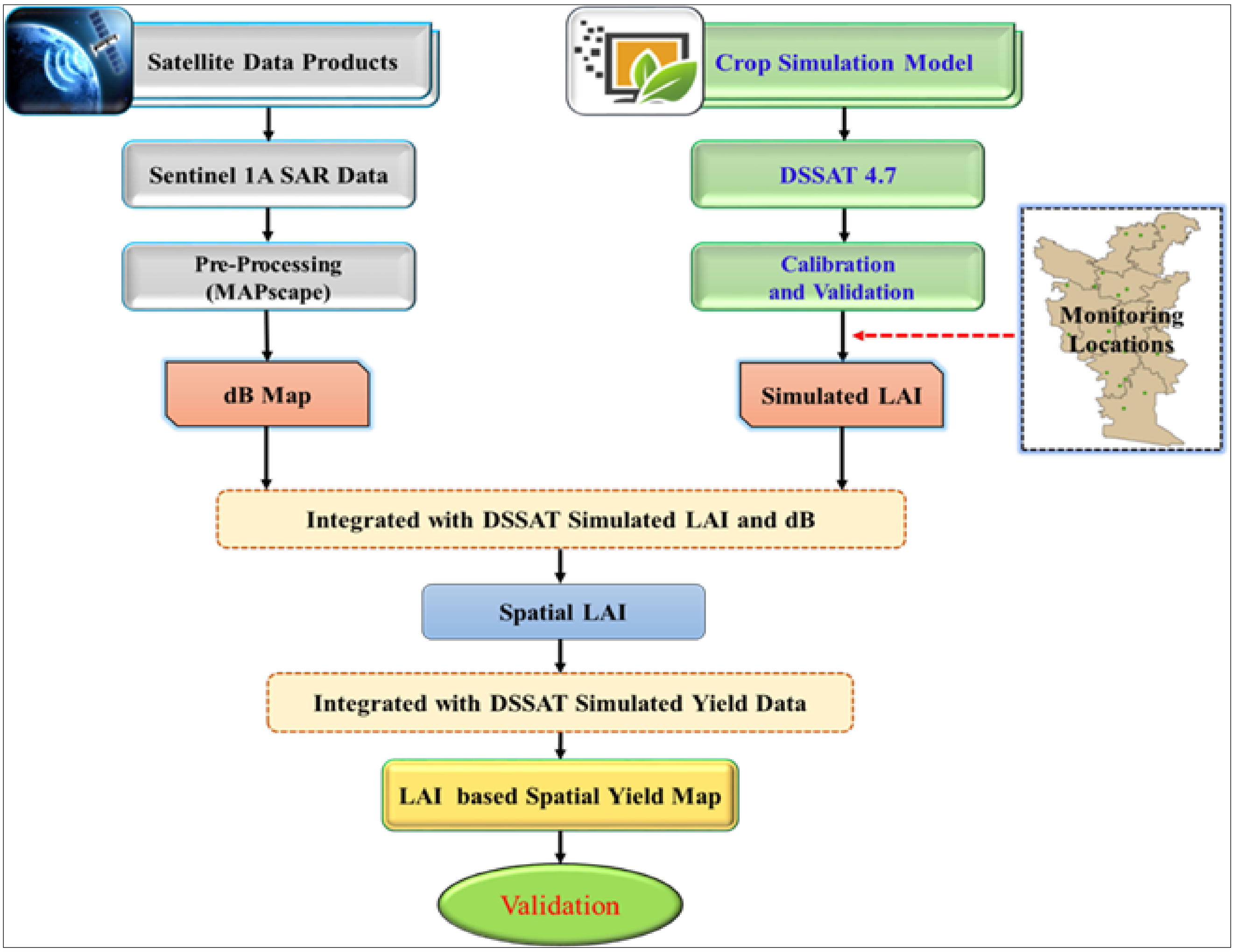

Fig. 3. Workflow for integrating SAR-based LAI with DSSAT-simulated yield for rice yield estimation.

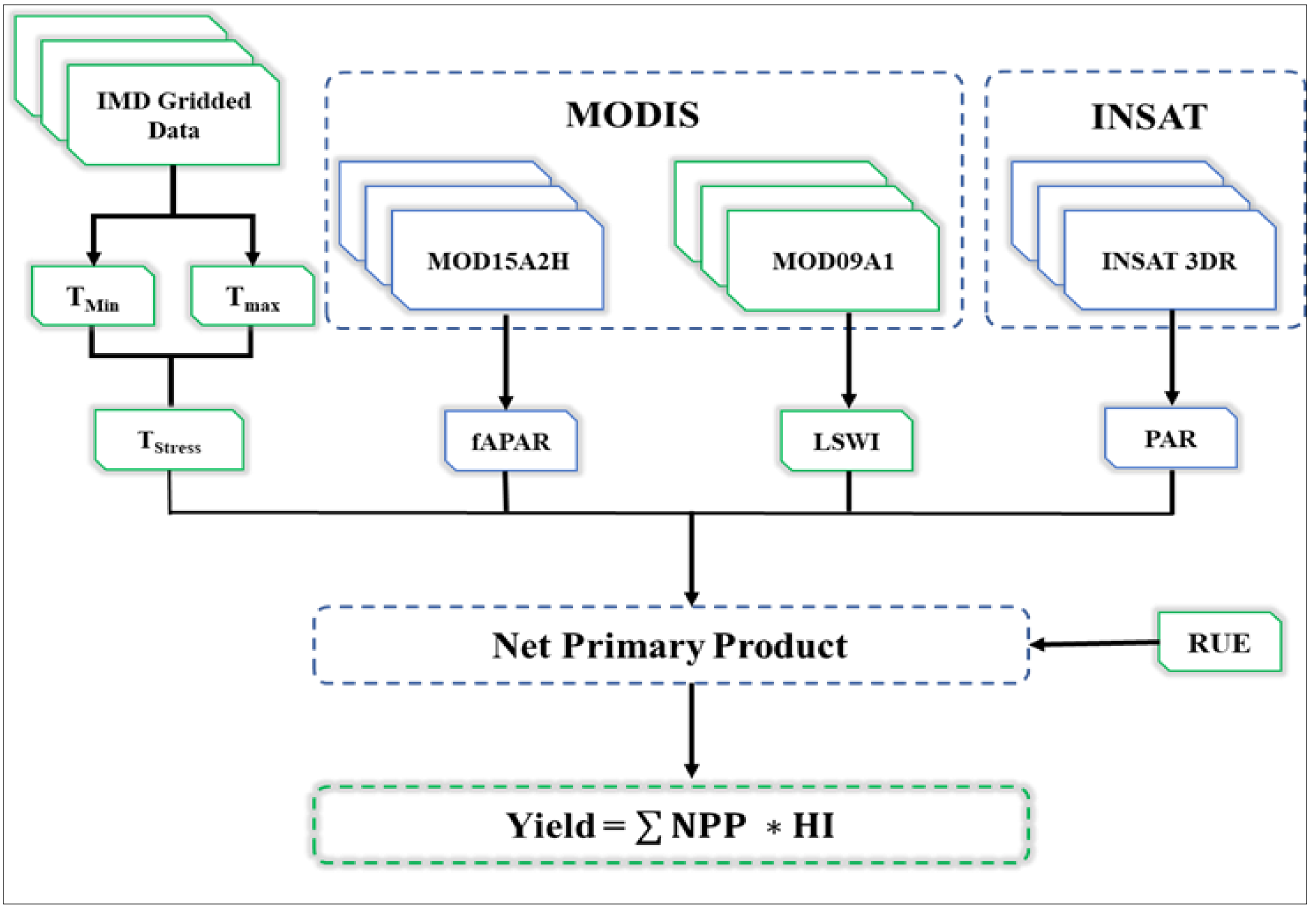

Fig. 4. Methodology for semi-physical approach yield estimation.

$$HI = \frac{\text{Economic Yield}}{\text{Bilogical Yield}} \quad \text{(Eqn. 5)}$$

Spatial rice yield estimation

Rice yield was calculated from the product of total NPP and harvest index of rice. The harvest index (HI) is the economic and biological yield ratio.

The spatial rice yield for the study area was calculated from the total NPP.

$$\text{Yield} = NPP_{sum} \times HI \quad \text{(Eqn. 6)}$$

Results and Discussion

Rice area estimation

Time-series Sentinel-1A SAR data were acquired for the period from August 2024 to January 2025. The data were pre-processed and analyzed using MAPscape software to estimate rice cultivation areas for the CDZ. The total rice area estimated across the entire study area was 298087 ha. Fig. 5 shows the spatial distribution of rice area across the CDZ. Among the four districts, Thanjavur recorded the highest rice sown area with 106914 ha, followed by Thiruvarur (101825 ha), Mayiladuthurai (45640 ha) and Nagapattinam (43708 ha) (Table 2). To assess the accuracy of the rice area classification, ground truth data were collected during the cropping season. A total of 182 rice points and 95 non-rice points were surveyed across the study area. The classification accuracy for rice area was found to be 93.90 %, with a Kappa coefficient of 0.88, indicating a high level of agreement between the classified and ground truth.

Table 2. District wise rice area during the *samba* season

S. No.	District	Rice area (ha)
1	Thanjavur	106914
2	Thiruvarur	101825
3	Nagapattinam	43708
4	Mayiladuthurai	45640
	Total	298087

Spatial yield estimation using the DSSAT model

Weather data

Weather input files for the crop simulation were generated using the DSSAT Weatherman utility for the CDZ. These datasets were critical inputs for the CERES-Rice model, capturing the temporal and spatial climatic variability during the rice-growing season. The generated weather files indicated a mean maximum temperature ranging from 27.9 °C to 35.8 °C and a mean minimum temperature between 20.6 °C and 25.8 °C across the districts. Additionally, solar radiation values varied slightly, from 13.4 to 21.7 MJ m^{-2} day^{-1}, indicating relatively consistent solar energy availability for photosynthesis during the growing period. Total seasonal rainfall recorded during the cropping period was 945 mm, highlighting spatial variability in water availability, a critical factor influencing rice growth and yield in the ecosystem.

Soil data

Soil input files for the CERES-Rice model were prepared using laboratory-analyzed data and formatted through the DSSAT 'SBuild' utility. The study area comprised 22 distinct soil series, highlighting the edaphic diversity of the CDZ. Soil texture varied widely, with sand ranging from 21.40 % to 85.90 %, silt 1.00 % to 29.60 % and clay 8.40 % to 54.10 %, leading to differences in water retention and infiltration. Bulk density ranged from 1.28 to 1.65 g cm^{-3} and organic carbon content ranging from 0.04 % to 1.43 %, indicating variability in soil fertility. These spatially explicit inputs were crucial for simulating yield variability and assessing soil-crop interactions within the model.

Calibration and validation

The CERES-Rice model in the DSSAT was calibrated to simulate rice growth and yield by incorporating variety-specific genetic coefficients. These coefficients were derived using the GENCALC utility for three predominant rice cultivars in the CDZ, namely, CR 1009, BPT 5204 and ADT 45 under uniform management and environmental conditions. The calibration process ensured accurate alignment of simulated phenological stages and yield with observed field data, thereby enhancing the model's reliability across spatially diverse conditions.

To enable spatial scaling of yield simulations, the remote sensing data is integrated with the crop simulation model. One of the critical steps in this process was the assimilation of remotely sensed LAI values derived from Sentinel-1A SAR imagery. Regression models were developed to relate SAR backscatter with field measured and model simulated LAI, allowing the extrapolation of LAI values across the entire study region. This spatially distributed LAI served as a driving variable in the model, providing a dynamic representation of crop canopy growth during the season. Using weather, soil, genetic and management inputs, along with spatially integrated LAI, the CERES-Rice model simulated key growth and development parameters. It includes days to emergence, anthesis and physiological maturity, as well as yield components such as biomass, harvest index and grain yield. The results indicated distinct spatial variability in simulated rice yields across the CDZ (Fig. 6). The mean rice yield for the entire study area was estimated at 3524 kg/ha. Among the districts, Thanjavur recorded the highest average yield of 3752 kg/ha, while Nagapattinam registered the lowest at 3330 kg/ha. Mayiladuthurai and Thiruvarur recorded intermediate yields of 3396 kg/ha and 3617 kg/ha, respectively, reflecting the influence of local agro-climatic and soil conditions on crop performance.

The results showed strong agreement between satellite -derived and observed yields, with district-level accuracy ranging from 85.50 % to 91.30 % and the overall agreement of the CDZ is 88.60 % (Table 3). Accurate simulation of growth stages and yield using CERES-Rice were reported, while NRMSE values of 11.38 % and 15.27 % for early and late rice cultivars were achieved, respectively (17, 18). Similarly, improved spatial yield predictions by integrating SAR-derived LAI with the DSSAT crop model was demonstrated (19).

Semi-physical model-based yield estimation

Net primary productivity (NPP) was estimated using key biophysical and environmental parameters, including PAR, FPAR, RUE and stress indices related to water and temperature (5). These components collectively represent the crop's ability to convert solar energy into biomass under varying environmental conditions.

Fig. 5. Spatial distribution of rice area for the Cauvery delta zone.

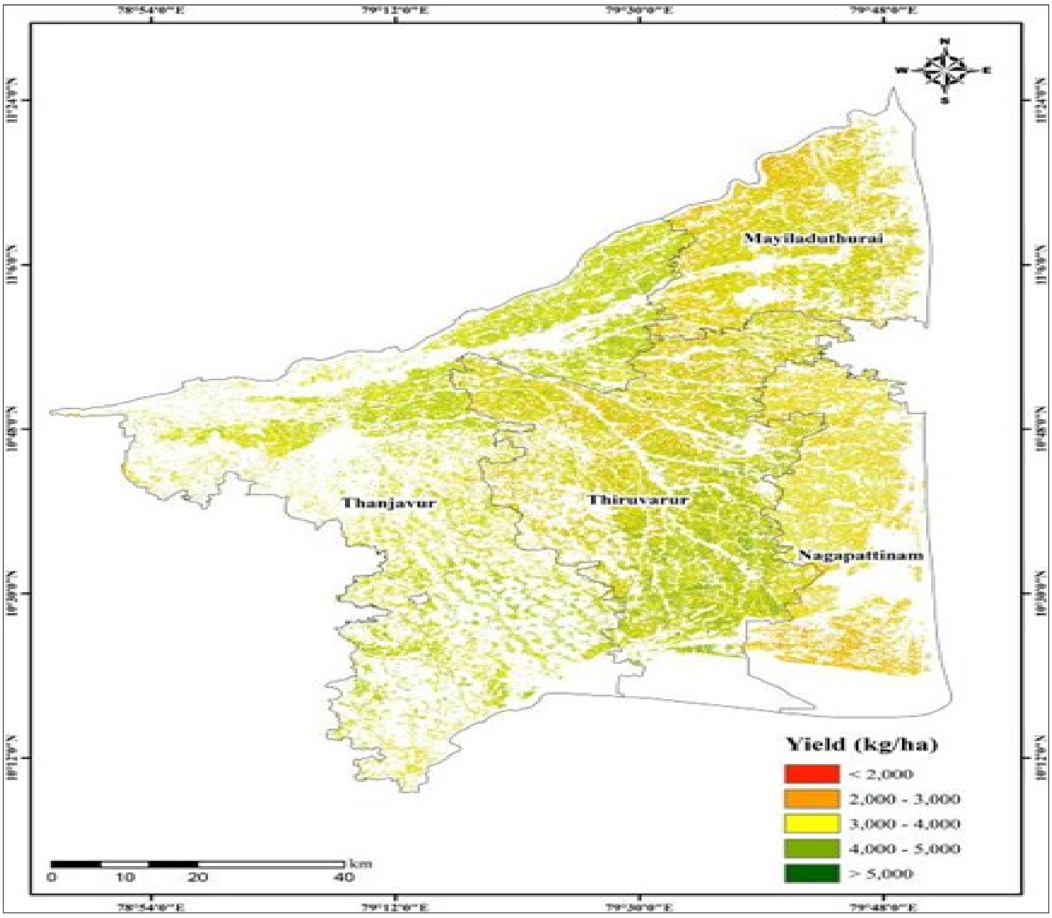

Fig. 6. DSSAT model based spatial rice yield.

PAR, which indicates the portion of solar radiation available for photosynthesis, varied seasonally from 150-315 MJ m^{-2}(5). Peak values (270–314 MJ m^{-2}) were recorded in September 2024 during active vegetative growth, while the lowest values (155–187 MJ m^{-2}) occurred in November 2024 due to cloud cover and reduced daylight during the reproductive and maturity stage. FPAR, representing canopy efficiency in capturing incident radiation, ranged from 0 to 1 across the season, reflecting dynamic changes in canopy structure and crop development. High FPAR values during mid-season coincided with vigorous vegetative growth. Water and temperature stress, key constraints to productivity, remained minimal throughout the rice-growing season in the CDZ due to adequate rainfall, irrigation and favourable temperatures, allowing for optimal photosynthesis and biomass accumulation. A constant RUE value of 2.9 g MJ^{-1} was used, as rice typically maintains stable RUE under optimal conditions (20).

The integration of PAR, FPAR, RUE and stress indices enabled spatial and temporal assessment of rice yield (Fig. 7). The average estimated yield was 4471 kg/ha, with the highest in Thiruvarur (4590 kg/ha), followed by Mayiladuthurai (4555 kg/ha), Thanjavur (4465 kg/ha) and Nagapattinam (4275 kg/ha). The semi-physical model achieved 83.30 % agreement with observed yields (Table 3). These results highlight the effectiveness of combining physiological parameters with environmental data to capture yield variability and support informed agricultural decision-making. Similar studies also estimated the yield using semi physical model (19, 21).

Comparison of DSSAT and semi-physical model based remote sensing yield

Spatial rice yield estimation using the DSSAT model and the semi-physical model (SPM) was compared against observed (CCE) data. The DSSAT-based yield estimates demonstrated a higher concordance with the observed values, achieving an accuracy of 88.60 %, whereas the SPM yielded a slightly lower accuracy of 83.60 % (Fig. 8). These results underscored the superior predictive capability of the DSSAT model when supplied with detailed input data.

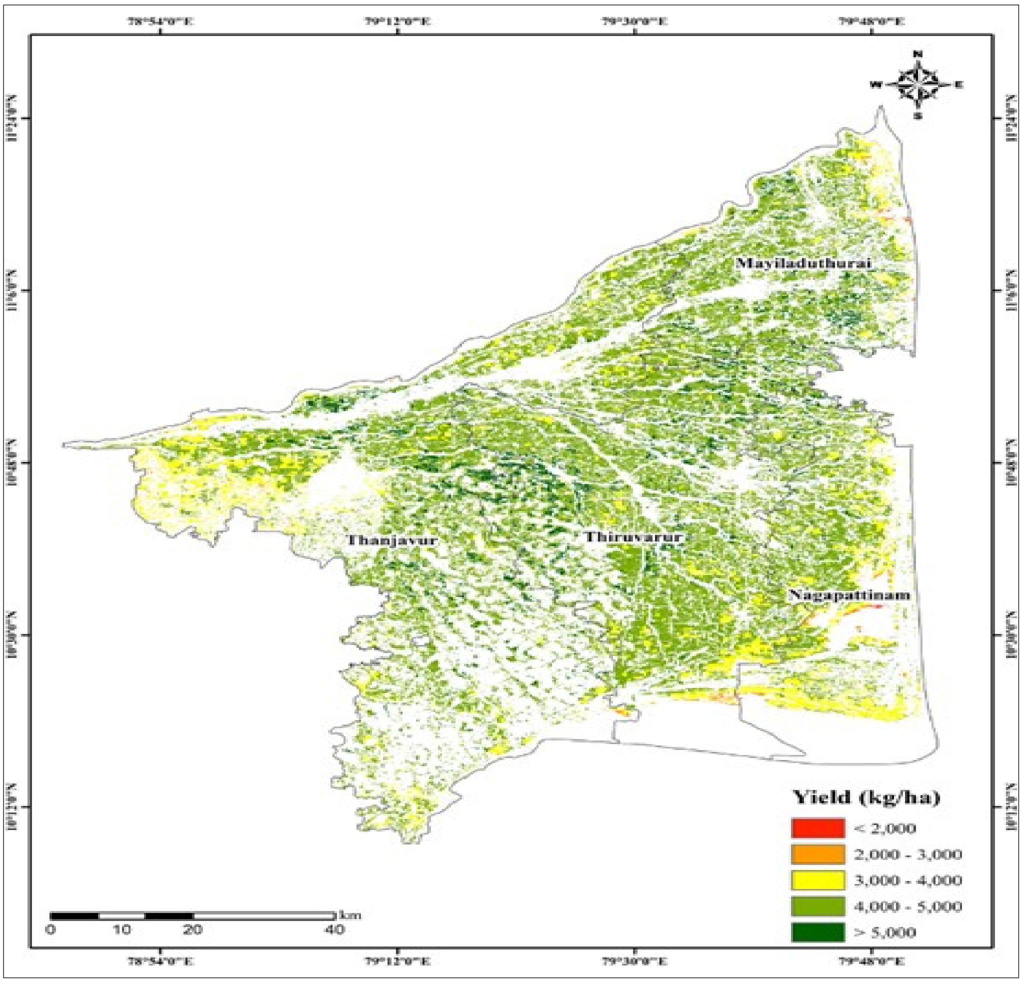

Fig. 7. Semi-physical model-based rice yield.

Table 3. Agreement between the observed yield and the different model based remote sensing yield

District	CCE (kg/ha)	SPM yield (kg/ha)	DSSAT yield (kg/ha)	Agreement between SPM and CCE Yield (kg/ha)	Agreement between DSSAT and CCE yield (kg/ha)
Mayiladuthurai	3597	3975	3355	84.40	87.60
Nagapattinam	3588	3897	3426	84.20	85.50
Thanjavur	3774	4379	3822	81.40	91.30
Thiruvarur	3624	4024	3689	83.40	90.10
Mean	3646	4068	3573	83.30	88.60

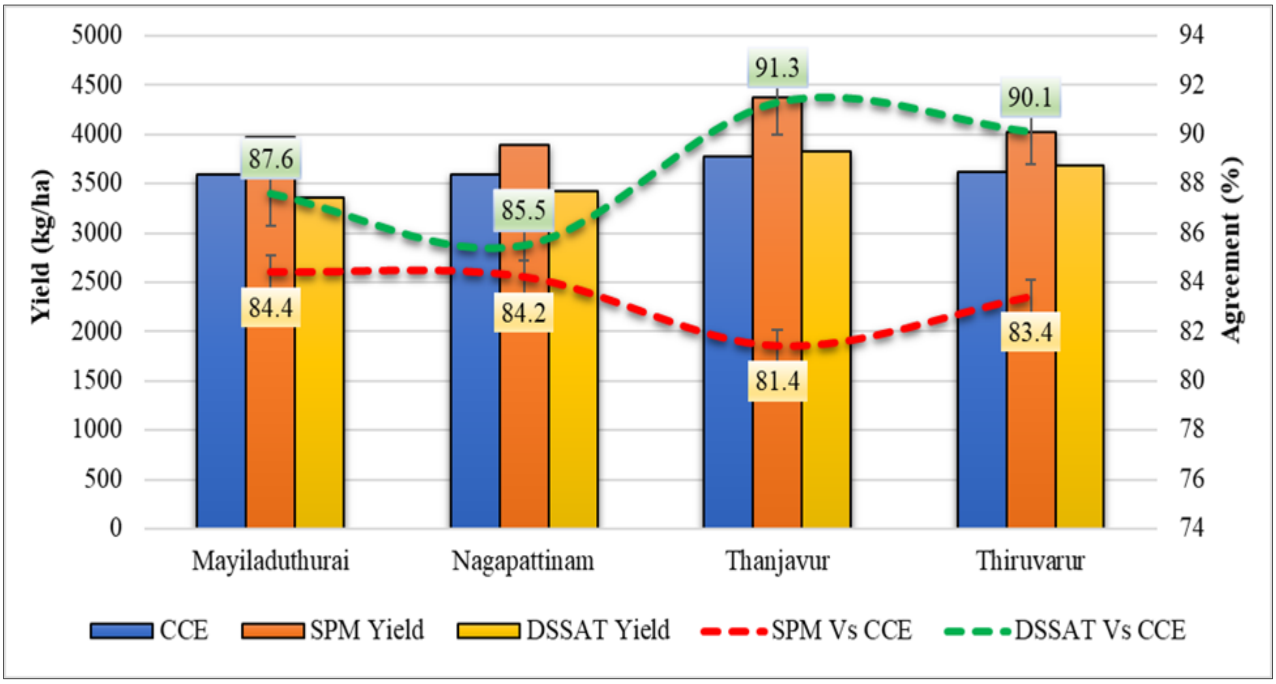

Fig. 8. Agreement between the observed yield and the different model yields.

The DSSAT model benefits from its ability to simulate complex interactions among soil, weather, crop genotype and management practices, resulting in more realistic and accurate yield predictions. However, the model's effectiveness is contingent upon the availability of extensive and precise input data, as well as considerable calibration efforts, which may limit its applicability in large-scale or time-sensitive scenarios. In contrast, the SPM, while slightly less accurate, offers a simpler and more scalable approach. It leverages remote sensing-derived parameters to estimate yield, making it useful in data-scarce environments. Yet, its reliance on empirical relationships and satellite data makes it more susceptible to input errors and environmental variability. In conclusion, while DSSAT offers higher prediction accuracy, it demands substantial data and calibration resources. The SPM, though relatively less accurate, presents a viable and operationally efficient alternative for regional-scale yield estimation, particularly in data-constrained settings.

Conclusion

The comparative evaluation of DSSAT and semi-physical models for spatial rice yield estimation in the CDZ has provided key insights into the capabilities and limitations of each approach. The DSSAT crop simulation model, calibrated with region-specific field data and integrated with SAR-derived LAI, demonstrated higher alignment with observed CCE data, achieving an accuracy of 88.60 %. This underscored the model's robustness in simulating crop growth under varying agro-climatic and soil conditions when supported by detailed input datasets. The semi-physical model, utilizing remote sensing-derived parameters such as PAR, FPAR, RUE and stress indices, offered a scalable and efficient alternative with an accuracy of 83.30 %. Its ability to estimate yield using fewer field inputs highlights its potential utility in operational contexts, particularly in data-scarce environments. However, its performance is more sensitive to input resolution and environmental variability. This study demonstrated the benefits of integrating advanced geospatial tools, simulation frameworks and biophysical modelling to improve regional scale rice yield estimation. The findings emphasized that while DSSAT excels in accuracy and depth of simulation, the semi-physical approach provides practical advantages in terms of scalability and ease of implementation. Together, these methodologies contribute to building a robust decision-support system for policymakers, agricultural planners and food security strategists, enabling timely and informed decisions across diverse rice-growing landscapes. The research reinforces the importance of adopting context-appropriate models to meet the dual objectives of accuracy and operational feasibility in agricultural monitoring, particularly under climate variability and resource constraints. Further, machine learning models can be integrated with either DSSAT or SPM for better accuracy.

Acknowledgements

We thank, the "MNCFC - Pilot Studies for GP level crop estimation using advanced technologies for non - cereal crops" project for providing fund conducting this research.

Authors' contributions

The conceptualization of the study was carried out by SS[1] and SP. Data processing was performed by KPR and NSS. Spatial analysis was conducted by SS[1] and APS. The methodology was developed by SS[1] and SP. Software support was provided by SS[2] and NSS. Supervision was undertaken by SP, DSK and DM. Visualization was handled by SS[1], SS[2] and NSS. The original draft was written by SS[1], while the review and editing of the manuscript were done by SS[2], NSS, RK, KPR and SP. All the authors significantly contributed to this study and have read and agreed to the published version of the manuscript. (SS[1] stands for S Satheesh and SS[2] stands for S Sakthivel)

Compliance with ethical standards

Conflict of interest: Authors do not have any conflict of interest to declare.

Ethical issues: None

Declaration of generative AI and AI-assisted technologies in the writing process : During the preparation of this work, the authors used ChatGPT by OpenAI to enhance language clarity and improve readability. After using this tool/service, the author reviewed and edited the content as needed and take full responsibility for the content of the publication.

References

1. Jabed MA, Murad MA. Crop yield prediction in agriculture: A comprehensive review of machine learning and deep learning approaches, with insights for future research and sustainability. Heliyon. 2024;10(24):e40836. https://doi.org/10.1016/j.heliyon.2024.e40836
2. Saleem A, Anwar S, Nawaz T, Fahad S, Saud S, Ur Rahman T, et al. Securing a sustainable future: The climate change threat to agriculture, food security and sustainable development goals. J Umm Al-Qura Univ Appl Sci. 2024;11:1-7. https://doi.org/10.1007/s43994-024-00177-3
3. Autio A, Johansson T, Motaroki L, Minoia P, Pellikka P. Constraints for adopting climate-smart agricultural practices among smallholder farmers in Southeast Kenya. Agric Sys. 2021;194:103284. https://doi.org/10.1016/j.agsy.2021.103284
4. Fang H, Liang S, Chen Y, Ma H, Li W, He T, et al. A comprehensive review of rice mapping from satellite data: Algorithms, product characteristics and consistency assessment. Sci Remote Sens. 2024;10:100172. https://doi.org/10.1016/j.srs.2024.100172
5. Jha MN, Kumar A, Dubey S, Pandey A. Yield estimation of rice crop using semi-physical approach and remotely sensed data. In: Jha CS, Pandey A, Chowdary V, Singh V, editors. Geospatial technologies for resources planning and management. Cham: Springer; 2022. p.1-15. https://doi.org/10.1007/978-3-030-98981-1_15
6. Mandapati R, Gumma MK, Metuku DR, Maitra S. Field-level rice yield estimations under different farm practices using the crop simulation model for better yield. Plant Sci Today. 2024;11(1):234-40. https://doi.org/10.14719/pst.2690
7. Parag M, Lottering R, Peerbhay K, Agjee N, Poona N. The use of synthetic aperture radar technology for crop biomass monitoring: A systematic review. Remote Sens Appl Soc Environ. 2024;33:101107. https://doi.org/10.1016/j.rsase.2023.101107
8. Holecz F, Barbieri M, Collivignarelli F, Gatti L, Nelson A, Setiyono TD, et al. An operational remote sensing based service for rice production estimation at national scale. In: Proceedings of the living planet symposium. 2013. https://dx.doi.org/10.13140/2.1.1492.8643
9. Aspert F, Bach-Cuadra M, Cantone A, Holecz F, Thiran JP. Time-varying segmentation for mapping of land cover changes. In: ENVISAT Symposium. 2007.
10. Nelson A, Setiyono T, Rala AB, Quicho ED, Raviz JV, Abonete PJ, et al. Towards an operational SAR-based rice monitoring system in Asia: Examples from 13 demonstration sites across Asia in the RIICE project. Remote Sens. 2014;6(11):10773-10812. https://doi.org/10.3390/rs61110773
11. Chaurasia G, Saxena S, Tripathy R, Chaudhari KN, Ray SS. Semi physical approach for sugarcane yield modelling with remotely sensed inputs. Vayu Mandal. 2017;43(1):11-22.
12. Liang S, Ma W, Sui X, Wang M, Li H. An assessment of relations between vegetation green FPAR and vegetation indices through a radiative transfer model. Plants. 2023;12(10):1927. https://doi.org/10.3390/plants12101927
13. Shao HB, Chu LY, Jaleel CA, Zhao CX. Water-deficit stress-induced anatomical changes in higher plants. Comptes Rendus Biologies. 2008;331(3):215-25. https://doi.org/10.1016/j.crvi.2008.01.002
14. Pai DS, Rajeevan M, Sreejith OP, Mukhopadhyay B, Satbha NS. Development of a new high spatial resolution (0.25 × 0.25) long period (1901-2010) daily gridded rainfall data set over India and its comparison with existing data sets over the region. Mausam. 2014;65(1):1-8. https://doi.org/10.54302/mausam.v65i1.851
15. Sigman DM, Hain MP. The biological productivity of the Ocean. Nature Edu Knowl. 2012;3(6):1-16.
16. Lake L, Guilioni L, French B, Sadras VO. Field pea. In: Sadras VO, Calderini DF, editors. Crop physiology case histories for major crops. Academic Press; 2021. p. 320-41. https://doi.org/10.1016/B978-0-12-819194-1.00009-8
17. Deka RL, Hussain R, Singh KK, Baxla A, Rao V, Balasubramaniyam R. Rice phenology and growth simulation using CERES-Rice model under the agro-climate of upper Brahmaputra valley of Assam. Mausam. 2016;67(3):591-98. https://doi.org/10.54302/mausam.v67i3.1374
18. Guo Y, Wu W, Bryant CR. Quantifying spatio-temporal patterns of rice yield gaps in double-cropping systems: A case study in pearl river delta, China. Sustain. 2019;11(5):1394. https://doi.org/10.3390/su11051394
19. Pazhanivelan S, Geethalakshmi V, Tamilmounika R, Sudarmanian NS, Kaliaperumal R, Ramalingam K, et al. Spatial rice yield estimation using multiple linear regression analysis, semi-physical approach and assimilating SAR satellite derived products with DSSAT crop simulation model. Agron. 2022;12(9):2008. https://doi.org/10.3390/agronomy12092008
20. Peng D, Huang J, Li C, Liu L, Huang W, Wang F, et al. Modelling paddy rice yield using MODIS data. Agric For Meteorol. 2014;184:107-16. https://doi.org/10.1016/j.agrformet.2013.09.006
21. Gumma MK, Nukala RM, Panjala P, Bellam PK, Gajjala S, Dubey SK, et al. Optimizing crop yield estimation through geospatial technology: A comparative analysis of a semi-physical model, crop simulation and machine learning algorithms. Agri Eng. 2024;6(1):786-802. https://doi.org/10.3390/agriengineering6010045

Additional information

Peer review: Publisher thanks Sectional Editor and the other anonymous reviewers for their contribution to the peer review of this work.

Reprints & permissions information is available at https://horizonepublishing.com/journals/index.php/PST/open_access_policy

Publisher's Note: Horizon e-Publishing Group remains neutral with regard to jurisdictional claims in published maps and institutional affiliations.

Indexing: Plant Science Today, published by Horizon e-Publishing Group, is covered by Scopus, Web of Science, BIOSIS Previews, Clarivate Analytics, NAAS, UGC Care, etc
See https://horizonepublishing.com/journals/index.php/PST/indexing_abstracting

Publisher information: Plant Science Today is published by HORIZON e-Publishing Group with support from Empirion Publishers Private Limited, Thiruvananthapuram, India.